GEOPHYSICAL RESEARCH LETTERS, VOL. 40, 423–428, doi:10.1029/2012GL053926, 2013

Satellite constraints of nitrogen oxide (NO_x) emissions from India based on OMI observations and WRF-Chem simulations

Sachin D. Ghude,[1,2] Gabriele G. Pfister,[2] Chinmay Jena,[1] R.J. van der A,[3] Louisa K. Emmons,[2] and Rajesh Kumar[2]

Received 18 September 2012; revised 27 November 2012; accepted 4 December 2012; published 22 January 2013.

[1] In this work, we map and develop for the first time an independent satellite constrained NO_x emission inventory for India for 2005 using an inverse technique and iterative procedure. We used OMI tropospheric NO_2 column retrievals over the Indian region, with tropospheric NO_2 columns simulated by the WRF-Chem model using the INTEX-B emission inventory. We determined the local relationship between modeled emissions and tropospheric columns and iteratively apply this relationship to OMI observations to derive an optimized NO*x* emission inventory on a 0.5°×0.5° grid. The optimized total NO_x emissions for India amount to 1.9 TgN/y and agree within 25% with EDGARv4.1 and the INTEX-B estimate. Our top-down inventory captures many of the missing hotspots in the original inventory and suggests that the INTEX-B inventory overestimates emissions over the Western and Eastern Indo-Gangetic region and underestimates point sources. We further evaluate the effect of the top-down inventory on surface ozone, which clearly indicates significant changes in spatial distribution. **Citation:** Ghude, S. D., G. G. Pfister, C. Jena, R. J. van der A, L. K. Emmons, and R. Kumar, (2012), Satellite constraints of nitrogen oxide (NO_x) emissions from India based on OMI observations and WRF-Chem simulations, *Geophys. Res. Lett.*, *40*, 423–428, doi:10.1029/2012GL053926.

1. Introduction

[2] Oxides of nitrogen (NO_x=NO+NO_2) are released into the atmosphere by natural (soils, lightning, etc.) as well as anthropogenic sources (fossil fuel combustion, biomass burning, etc). It is believed that anthropogenic NO_x emissions surged simultaneously with large-scale urbanization, industrialization, and economic growth in India and attracted the attention of researchers and policy makers [*Garg et al*., 2001; *Ghude et al*., 2008]. Thermal power plants are the largest consumer of coal in India [*Garg et al*., 2001]. Energy and industrial sector is estimated to be the largest contributor to India's NO_x emissions (~50%) followed by the transportation sector (~35%) [*Garg et al*., 2001].

[3] To obtain a better understanding on how NO_x emissions from this region influence air pollution on regional and global scale, accurate information on the NO_x emissions budget on spatial and temporal scales is essential [*Kunhikrishnan et al*., 2004]. In recent years, NO_x emission inventories and NO_x budgets for India/Asia have been estimated using traditional bottom-up approaches integrating information about emission source types, fuel consumption, and source specific emission factors. For example, *Garg et al*. [2001] developed a NO_x emission inventory for India on a district level, whereas the Intercontinental Chemical Transport Experiment-Phase B (INTEX-B), the Emission Database for Global Atmospheric Research (EDGAR), and the Regional Emission inventory in Asia (REAS) were developed to provide emissions on 0.5°×0.5° horizontal resolution [*Streets et al*., 2003; *Ohara et al*., 2007; *Zhang et al*., 2009]. However, these estimates are considered highly uncertain due to limited/lack of access to information on specific sources, lack of accurate statistics on the source data and process technology, inaccurate information on the locations of specific sources, and missing information on source specific emission factors for India. This poses a limit for developing accurate NO_x emissions, leads to discrepancies between modeled and satellite NO_2 column [*Kumar et al*., 2012], and is a shortcoming for studies on surface ozone over India [*Deb Roy et al*., 2009]. Validation of NO_x emissions and spatial allocation of its sources with independent measurements is still an outstanding issue for India.

[4] Retrievals of tropospheric NO_2 column from satellite instruments (e.g. GOME, SCIAMACHY, and OMI) provide valuable data for identifying and evaluating NO_x emissions from surface sources [*Leue et al*., 2001, *Martin et al*., 2003; *Lamsal et al*., 2011]. *Martin et al*. [2003] described an inverse based top-down approach to estimate NO_x emissions on a global scale using tropospheric NO_2 retrievals from GOME. With the improvement of the spatio-temporal resolution of satellite observations, recent inverse studies have attempted to derive top-down constraints of NO_x emissions using chemical transport models on regional scales [*Zhao and Wang*, 2009; *Lin*, 2012].

[5] Most inverse estimates were either derived for global scales or focused on North America or China, and no such estimates have been attempted for the Indian region. In this work, for the first time, we aim to map and derive independent NO_x emissions for India on 0.5°×0.5° horizontal resolution based on OMI observations and WRF-Chem simulations. Our estimate provides useful firsthand information to modelers and policymakers about current air pollution sources and allow for examining future mitigation strategies. We follow the method used in *Martin et al*. [2003] and *Kuenen* [2006] to derive total NO_x emissions for January 2005. We also evaluate the effect of the newly developed inventory on the distribution of surface ozone over the India region.

[1]Indian Institute of Tropical Meteorology, Pune, India.
[2]Atmospheric Chemistry Division, National Center for Atmospheric Research, USA.
[3]Royal Netherlands Meteorological Institute, De Bilt, Netherlands.

Corresponding author: Sachin D. Ghude, Indian Institute of Tropical Meteorology, Pune, India. (sachinghude@tropmet.res.in)

0094-8276/13/2012GL053926

2. Methodology

2.1. Satellite Data

[6] OMI aboard Aura observes the atmosphere in nadir viewing geometry with a local equator crossing time between 13:40 and 13:50 LT. The KNMI-DOMINO product provides a tropospheric NO_2 column dataset and is available at www.temis.nl. In brief, tropospheric NO_2 column is derived in three main steps involving the calculation of (1) slant column (using Differential Optical Absorption Spectroscopy (DOAS) approach in the 405–465 nm spectral window), (2) tropospheric slant column (using modeling/assimilation approach), and (3) tropospheric vertical column (using air mass factor—AMF). OMI retrieval errors have an absolute component of ~1.0×10^{15} molecules/cm^2 and a relative AMF component of 25% [*Boersma et al.*, 2011]. More details on the retrievals and error budgets are discussed by *Boersma et al.* [2011]. In this work, we use daily level-2 (Version 2.0) data from DOMINO with solar zenith angles <80º, cloud radiance fraction less than 50%, and cloud fraction less than 0.2. In addition, we exclude pixels corresponding to viewing angle exceeding 45° (pixels at the edge of swath).

2.2. WRF-Chem Model

[7] The study uses the Weather Research and Forecasting model coupled with Chemistry(WRF-Chem) version 3.2.2 covering a domain of south Asia at 0.5°×0.5° horizontal resolution (~55 km×55 km) to simulate tropospheric NO_2 columns for the month of January 2005. The model uses MOZART-4 gas phase chemistry linked to the GOCART aerosol scheme and is driven by NCEP/FNL meteorological reanalysis fields (GFS/NFL) as provided by NCAR (http://rda.ucar.edu/datasets/ds083.2/). We use grid nudging to constrain the large flow in the model to the analysis fields. The initial and boundary conditions for the chemical fields are updated every 6 h, based on the MOZART-4 simulations [*Emmons et al.*, 2010], and WRF-Chem outputs are every hour. Biogenic emissions of trace species are calculated online using the Model of Emissions of Gases and Aerosols from Nature (MEGAN) [*Guenther et al.*, 2006]. Anthropogenic emissions of CO, NO_x, SO_2, NMVOC, PM10, PM2.5, and BC/OC are taken from the INTEX-B inventory [*Zhang et al.*, 2009], including sources from power plants, industry, transportation, and the residential sector. Soil NO_x emissions are calculated by the MEGAN model in WRF-Chem, and the simulations did not include aircraft or lightning NO_x emissions. Emissions from biomass burning are provided to the model via the Fire Inventory from NCAR version-1(FINNv1) [*Wiedinmyer et al.*, 2011].

[8] For consistency with satellite retrievals, model output at each day is interpolated in time and space to locations of valid satellite retrievals and convolved with the averaging kernels used in the DOMINO retrievals as described in the OMI/DOMINO User's Guide (http://www.temis.nl/docs/OMI_NO2_HE5_2.0_2011.pdf) and by *Kumar et al.* [2012]. The daily data are averaged to obtain a monthly mean value for each 0.5°×0.5° grid box.

3. Results

3.1. Comparison Between OMI and WRF-Chem Simulated Tropospheric Column NO_2

[9] Figure 1 shows the OMI tropospheric NO_2 columns for January 2005. The spatial pattern of OMI NO_2 (Figure 1) illustrates larger Tropospheric Vertical Column Densities (TVCDs) (>4.5×10^{15} molecules/cm^2) in regions of industrial activities and/or dense population, including the Eastern and Western Indo-Gangetic (IG) region and the Mumbai-Gujarat Industrial Corridor(MGIC). High values are also evident over individual large thermal power plants and big cities. The reader can refer to *Ghude et al.* [2008] for a detailed analysis of emission hotspots in India.

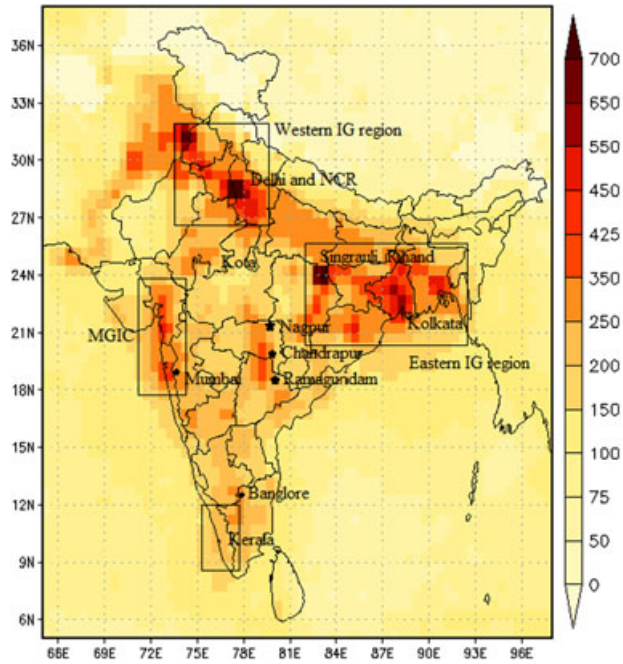

Figure 1. OMI tropospheric NO_2 column (×10^{13} molecules/cm^2) for January 2005 over Indian region.

[10] Figure 2 (left) shows the WRF-Chem tropospheric NO_2 columns and compares (Figure 2 right) OMI and WRF-Chem tropospheric NO_2 columns for January 2005. WRF-Chem overall captures the spatial features of retrieved TVCDs such as higher values over the IG region and lower values over the central and far northeastern region of India. However, it shows poor agreement for specific spatial features (Figure 2a). Spatial correlation between modeled and retrieved TVCDs (R^2) is found to be 0.68. The spatial discrepancies between modeled and OMI tropospheric column NO_2 is further illustrated by the OMI-minus-WRF differences shown in Figure 2b. WRF-Chem overestimates the magnitude of retrieved tropospheric NO_2 column over most of the study domain; the IG region is overestimated by about 30–120%. Modeled NO_2 columns are also higher than OMI measurements over the southern tip (Kerala) of India. On the other hand, modeled NO_2 columns are significantly lower than OMI measurements by about 1.2–2.8×10^{15} molecules/cm^2 (30–70%) over the MGIC region. The model also tends to underestimate OMI retrievals by about 1.2–1.8×10^{15} molecules/cm^2 (20–50%) over the large capacity thermal power plants situated at Chandrapur, Nagpur, and Ramagundam, and by about 2.8×10^{15} molecules/cm^2 (80%) over the high-capacity thermal power plants at Singrauli. The observed discrepancies between simulated and observed tropospheric NO_2 column are consistent with results from

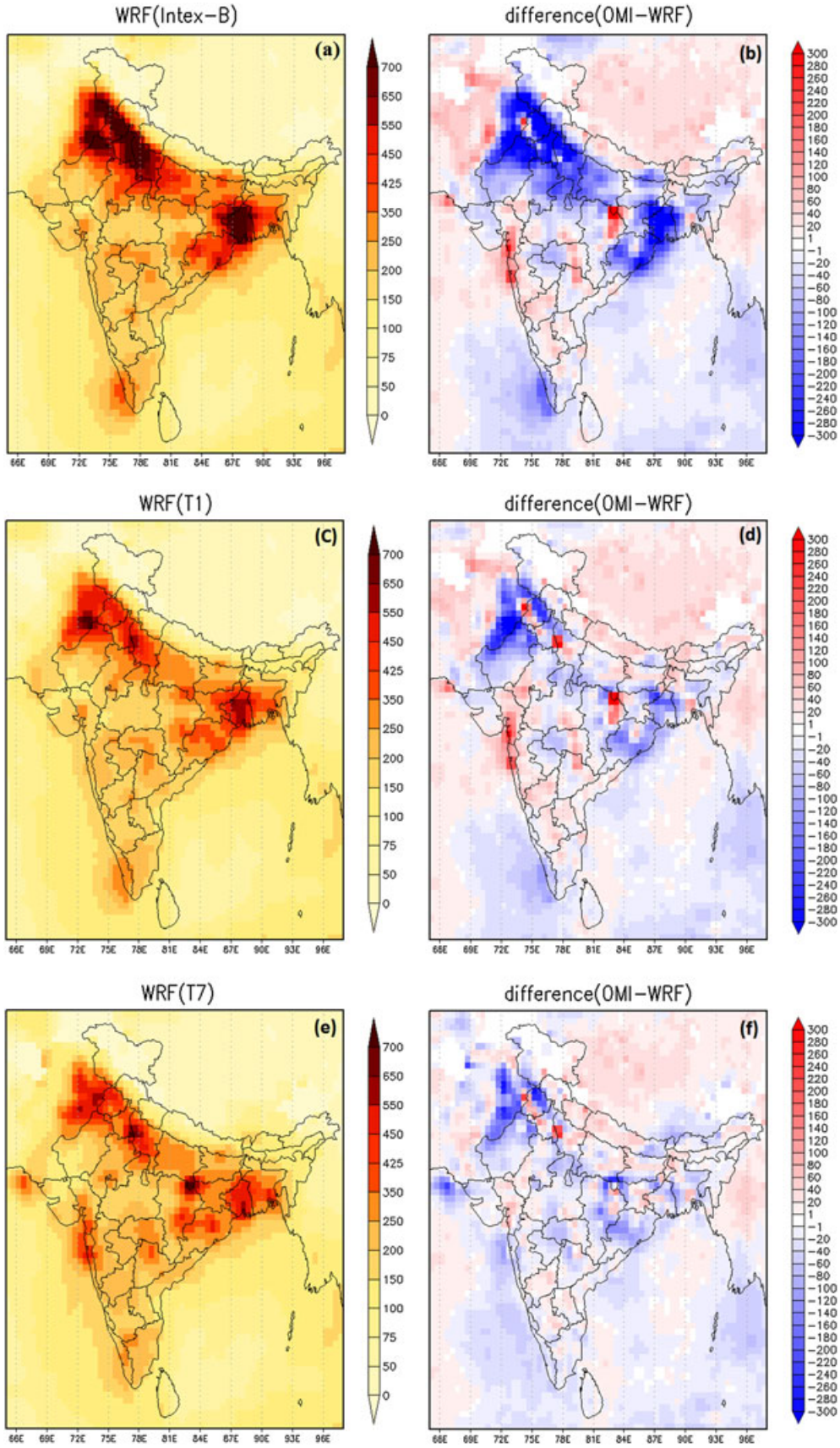

Figure 2. (a) WRF-Chem tropospheric NO_2 column for January 2005 and difference (OMI—WRF-Chem) for simulations using the INTEX-B inventory (top panel), a first iteration of the top-down estimate (middle panel) and a final optimized top-down estimate (bottom panel). WRF-Chem profiles are convolved with OMI averaging kernels before comparison. *Tropospheric column NO_2 unit is* 10^{13} *molecules/cm*^{2}*/s*.

previous studies over India (*Kunnikrishnan et al.*, 2004; *Kumar et al*., 2012). These differences point to general overestimation of anthropogenic NO_x emissions in the regions where the model overestimates the observed TVCDs and underestimation of NO_x emissions in the regions where modeled values are significantly lower than observed values [*Kumar et al*., 2012]. Another possible source of difference can arise from errors in simulating tropospheric NO_x chemistry [*Martin et al.,* 2003; *Valin et al*., 2011] and non-anthropogenic emission sources including soil NO_x, lightning, or biomass burning. The influence of fires, however, is small during January.

3.2. Inversion of OMI Observations (Top-Down Approach)

[11] Tropospheric NO_2 columns are strongly related to surface NO_x emissions because of its short lifetime. Neglecting horizontal transport and assuming a linear relationship between NO_x emissions and NO_2 column, an estimate of the top-down NO_x emission, E, can be inferred through the following mass balance relation:

$$E = (E_{\mathrm{NOx}}/T_{\mathrm{NO2}})^{*}\mathrm{OMI}_{\mathrm{NO2}} \quad (1)$$

[12] E_{NOx} represents the a priori NO_x emissions (here INTEX-B), T_{NO2} the tropospheric NO_2 column obtained from the model simulation and convolved with the OMI averaging kernels, and $\mathrm{OMI}_{\mathrm{NO2}}$ the TVCD. Using the modeled $E_{\mathrm{NOx}}/T_{\mathrm{NO2}}$ ratio in equation (1), we perform an inversion to derive a first top-down estimate (called "a posteriori" in the following) for NO_x emissions for each $0.5°\times0.5°$ grid box. The a posteriori emissions from the first iteration are then used in the model to simulate updated NO_2 columns.

[13] Figures 1c and 1d show the simulated NO_2 columns with a posteriori emission (WRF(T1)) and the difference between observed and modeled NO_2 columns, respectively. The agreement with OMI observations clearly improved, particularly over the IG region. The R^2 for the spatial correlation between modeled and retrieved TVCDs increased to 0.76. However, modeled NO_2 columns are still significantly lower than OMI measurements (by about 30–70%) over the MGIC region, high-capacity thermal power plants, and other hotspots.

[14] To further improve the agreement between modeled and observed tropospheric NO_2 columns, we follow the iterative procedure described in Kuenen [2006]. We calculate a new $E_{\mathrm{NOx}}/T_{\mathrm{NO2}}$ ratio using the WRF(T1) simulation and again re-estimated NO_x emissions following equation (1). This process is repeated until the difference between simulated and observed tropospheric NO_2 columns is less than ±10% over most of the hotspots regions. In this case, the iteration has been performed seven times.

[15] The final comparison between modeled and observed tropospheric TVCDs is shown in Figures 1e and 1f. Simulated NO_2 columns now show better agreement with OMI retrievals, particular over the IG region, emission hotpots, and the southern tip of India. The R^2 value for the spatial correlation between modeled and retrieved TVCDs is now increased to 0.88. The difference between simulated and observed NO_2 columns is within ±10–15%, except for a small region in the northwestern part of India (Panjab) and eastern Pakistan where simulated TVCDs are higher by about $0.8–2.2\times10^{15}$ molecules/cm^2 (20–80%). Model simulations using the final a posteriori emissions now reflect the localized enhancement in NO_2 columns in Northeastern India and the national capital region (surrounding Delhi). There is also a significant increase in simulated NO_2 columns and better agreement with OMI over the city of Mumbai, the MGIC region, and high-capacity thermal power plants. This suggests that surface NO_x emissions from these locations are significantly underestimated in the INTEX-B inventory and that the optimized top-down inventory provides a much more accurate estimate of the actual emissions sources.

3.3. Comparison Between INTEX-B and Final Top-Down Emissions

[16] Figures 3a and 3b show the spatial distribution of NO_x emissions for INTEX-B and the optimized top-down inventory, respectively, and Figure 3c shows the difference. The R^2 value for the spatial correlation between INTEX-B and top-down emission is poor (0.20) indicating significant deviation between these two emission estimates. The largest differences in Figure 3c are seen over the densely populated regions of India, over big cities or over the locations of thermal power plants and industrial sites. The optimized top-down inventory is more localized and captures more hotspots sources compared to INTEX-B. The a posteriori total NO_x emissions for 2005 over India amount to 1.9 TgN, compared to 2.4 TgN in EDGARv4.1 (http://edgar.jrc.ec.europa.eu/) and 2.1 TgN (for 2006) in INTEX-B. As seen from Figure 3, INTEX-B overestimates NO_x emissions for most of the Indo-Gangatic (IG) region, where the rural population density is highest, and industrial/vehicular sources are dominant. Similar overestimation in INTEX-B emissions is also evident in the densely populated southern tip (Kerala) of India. In contrast, significant underestimation of NO_x emissions (more than $2.2\mathrm{x}10^{11}$ molecules/cm^2/s) over Mumbai, the MGIC region, high-capacity power plant sources (e.g., Chandrapur, Nagpur, Ramagundam, Singrauli, Talcher), and other point sources are evident in INTEX-B. Therefore, the overall estimate in INTEX-B is comparable with the top-down estimate.

[17] We do not attempt to provide a quantitative estimate of the uncertainty in the magnitude of our top-down estimate. However, it should be noted that the top-down estimate E is subject to various sources of uncertainty including uncertainties in OMI retrievals [*Boersma et al*., 2011] and the model simulations [*Kumar et al*., 2012], and nonlinearity between emission of NO_x and column NO_2 due to NO_x transport between the grid cells [*Martin et al*., 2003, *Kuenen*, 2006]. Uncertainty due to transport between the grid cells is expected to be small because the iteration process compensates for transport to neighboring grid cells [*Kuenen*, 2006]. Averaged over India, the magnitude of simulated NO_2 columns (with optimized inventory) is about 10% higher than observed by OMI. The overall error for individual retrieved tropospheric column NO_2 is reported as ~25% plus 1.0×10^{15} molecules/cm^2 in DOMINO version 2.0 retrievals [*Boersma et al*., 2011]. Even though the usefulness of the optimized top-down estimate is limited by these uncertainties, it provides useful information about trends and spatial coverage to policymakers and air quality modelers. The significant improvement specifically in the spatial allocation is demonstrated by comparison to demographic information.

3.4. Change in Surface Ozone Distribution

[18] In this section, we analyze the impact of the optimized top-down inventory on the spatial distribution of surface O_3

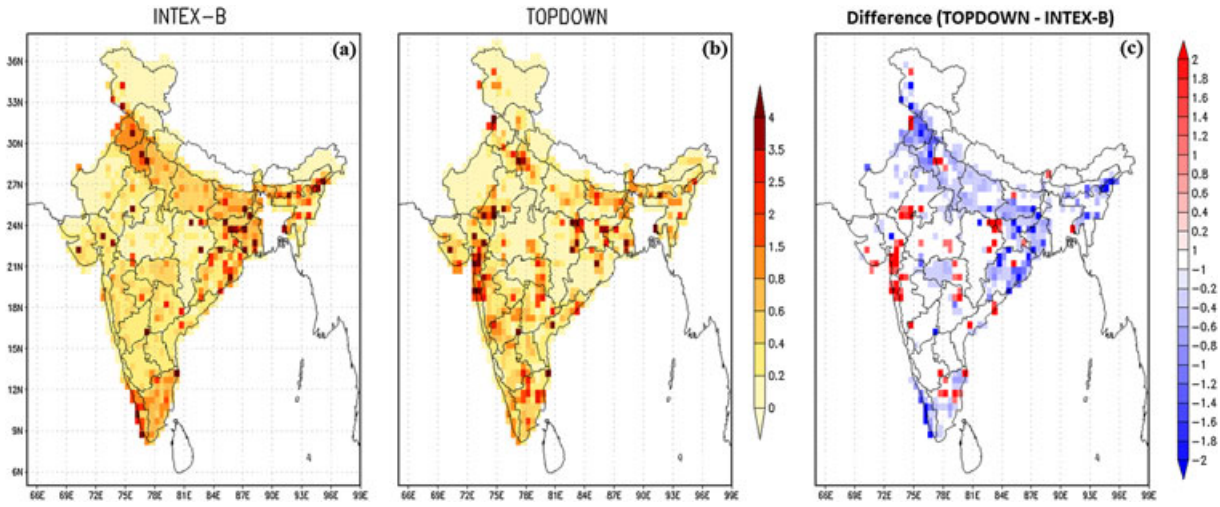

Figure 3. Spatial distribution of NO_x emission from (a) INTEX-B inventory and (b) optimized top-down inventory, and (c) their difference (*emission unit is* 10^{11} *NO molecules/cm*^{2}*/s*).

over the India region. Except for anthropogenic NO_x, no other emissions have been updated in the model. Figure 4 compares the monthly mean of daily maximum surface ozone simulated using the optimized top-down and the INTEX-B inventory for January 2005, respectively. A notable change in the O_3 distribution is seen, particularly over outflow regions such as the Arabian Sea or the Bay of Bengal but also over large emission hotspots. The top-down inventory leads to a significant decrease in surface O_3 of about 8–14 ppb (from ~50–58 ppb with Intex-B to ~42–46 ppb with top-down inventory) over the MGIC region and an increase of the same order over the Arabian Sea. Significant increase in NO_x emissions (from ~8–15 ppb with Intex-B to ~18–27 ppb with top-down inventory) from these areas (about 10×10^{11} molecules/cm^2/s, about 10–12 ppb for surface NO_2) results in more titration of O_3 during daytime but enhanced production in the downwind region. On the other hand, surface ozone decreases (from ~58–70 ppb with Intex-B to ~50–58 ppb with top-down inventory) on average by about 8–12 ppb downwind of the southern tip of India (Kerala). This is consistent with the decrease in NO_x emission (about $1–5\times10^{11}$ molecules/cm^2/s, about 4–7 ppb for surface NO_2) from this region (from ~12–18 ppb with Intex-B to ~8–11 ppb with top-down inventory), which results in reduced O_3 production downwind. Surface O_3 also decreases (~2–8 ppb) over the Bay of Bengal as a result of reduced NO_x emissions from Northeastern India. The significant reduction of NO_x top-down emissions for the Western IG region leads to an increase in surface O_3 of the order of 2–6 ppb in this region possibly due to less titration of O_3 by NO_x compared to the INTEX-B simulation. These results show the large sensitivity of modeled surface ozone not only to the magnitude of the emissions but the location of the NO_x emission source itself. These results potentially have important implications for urban and industrial areas where emission control policies are implemented or proposed.

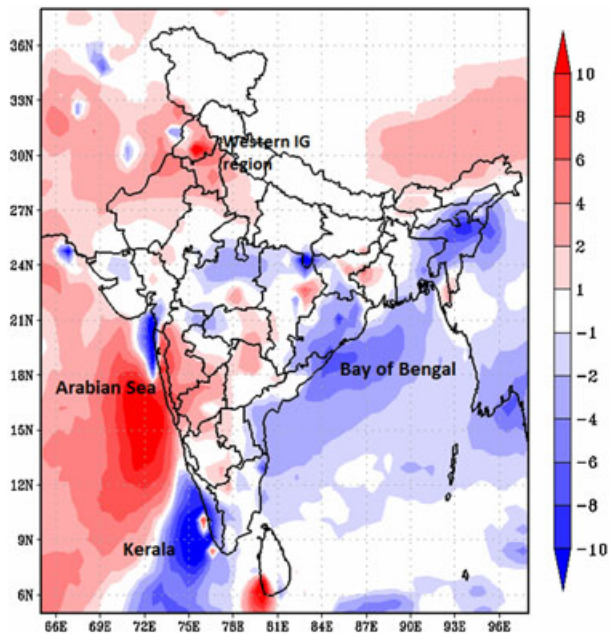

Figure 4. Change in surface ozone (ppbv) for WRF-Chem simulations using optimized top-down inventory minus simulations using the INTEX-B inventory.

4. Conclusions

[19] Accurate NO_x emissions are essential for air pollution quantification and mitigation. In this paper, for the first time we have mapped and derived an independent NO_x emission estimate for India based on OMI tropospheric NO_2 retrievals and the WRF-Chem model using an iterative inverse technique. The overall total NO_x emissions for India in 2005 amount to 1.9 TgN yr^{-1}, comparable with the estimate of 2.4 TgN yr^{-1} in EDGARv4.1 and 2.1 TgN yr^{-1} (for 2006) in the INTEX-B inventories. However, we found that there is in general an overestimation of NO_x emissions in the INTEX-B inventory for the Western and an Eastern IG region and the Southern tip of India (Kerala), as well as underestimation over large power plants, cities, and MGIC region. Significant changes in the modeled spatial distribution of daytime maximum O_3 are seen when the optimized top-down inventory is used instead of the INTEX-B inventory. These results may have important policy implications for

urban/industrial areas in India where NO_x emissions are already high and expected to increase in the future with impending demands of energy. While there are still remaining uncertainties in our top-down estimate, this method provides a potential basis for mapping and evaluating robust independent NO_x emissions and trends, particularly for regions with large uncertainties such as India, and provides important information to air quality modelers and policy makers. This inventory data set is available online at http://www.tropmet.res.in/emission/.

[20] **Acknowledgments.** This work is supported by the Department of Science and Technology, Government of India under the BOYSCAST fellowship program. We wish to thank B.N. Goswami (Director, IITM), Randall Martin (Dalhousie University) and Bas Mijling (KNMI) for encouraging the discussions. NCAR is operated by the University Corporation of Atmospheric Research under sponsorship of the National Science Foundation.

References

Boersma, K. F., et al. (2011), An improved retrieval of tropospheric NO_2 columns from the Ozone Monitoring Instrument, *Atmos. Meas. Tech*, *4*, 1905–1928.

Deb Roy, S., G. Beig, and Sachin D. Ghude (2009), Exposure-plant response of ambient ozone over the tropical Indian region, *Atmos. Chem. Phys 9*, 5253–5260.

Emmons, L. K., et al. (2010), Description and evaluation of the Model for Ozone and Related chemical Tracers, version 4 (MOZART-4), *Geosci. Model Dev 3*, 43–67.

Garg, A., P. R. Shukla, S. Bhattacharya, and V. K. Dadhwal (2001), Sub-region (district) and sector level SO_2 and NO_x emissions for India: Assessment of inventories and mitigation flexibility, *Atmos. Environ. 35*, 703–713.

Ghude, S. D., S. Fadnavis, G. Beig, S. D. Polade, and R. J. van der A (2008), Detection of surface emission hot spots, trends, and seasonal cycle from satellite-retrieved NO_2 over India, *J. Geophys. Res. 113*, D20305, doi:10.1029/2007JD009615.

Guenther, A., T. Karl, P. Harley, C. Wiedinmyer, P. I. Palmer, and C. Geron (2006), Estimates of global terrestrial isoprene emissions using MEGAN (Model of Emissions of Gases and Aerosols from a Nature, *Atmos. Chem. Phys 6*, 3181–3210.

Kuenen, J. J. P., Anthropogenic NO_x emission estimates for China based on satellite measurements and chemistry-transport modelling Technical report: 2006, KNMI, Technical Report, 62p.

Kumar, R., M. Naja, G. G. Pfister, M. C. Barth, C. Wiedinmyer, and G. P. Brasseur (2012), Simulations over South Asia using the weather research and forecasting model with chemistry (WRF-Chem): Chemistry evaluation and initial results, *Geosci. Model Dev.*, *5*, 619–648.

Kunhikrishnan, T., et al. (2004), Analysis of tropospheric NO_x over Asia using the model of atmospheric transport and chemistry (MATCH-MPIC) and GOME-satellite observations, *Atmos. Environ.*, *38*, 581–596.

Lamsal, L. N., et al. (2011), Application of satellite observations for timely updates to global anthropogenic NO_x emission inventories, *Geophys. Res. Lett.*, *38*, L05810, doi:10.1029/2010GL046476.

Leue, C., M. Wenig, T. Wagner, U. Platt, and B. Jahne (2001), Quantitative analysis of NO_x emissions from GOME-satellite image sequences, *J. Geophys. Res.*, *106*, 5493–5505.

Lin, J. T. (2012), Satellite constraint for emissions of nitrogen oxides from anthropogenic, lightning and soil sources over East China on a high-resolution grid, *Atmos. Chem. Phys.*, *12*, 2881–2898.

Martin, R. V., D. J. Jacob, K. Chance, T. P. Kurosu, P. I. Palmer, and M. J. Evans (2003), Global inventory of nitrogen oxide emissions constrained by space-based observations of NO_2 columns, *J. Geophys. Res.*, *108*(D17), 4537–4548.

Ohara, T., H. Akimoto, J. Kurokawa, N. Horii, K. Yamaji, X. Yan and T. Hayasaka (2007), An Asian emission inventory of anthropogenic emission sources for the period 1980–2020, *Atmos. Chem. Phys.*, *7*, 4419–4444.

Streets, D. G., et al. (2003), An inventory of gaseous and primary aerosol emissions in Asia in the year 2000, *J. Geophys. Res.*, *108*, doi:10.1029/2002JD003093.

Valin, L. C., A. R. Russell, R. C. Hudman, and R. C. Cohen (2011), Effects of model resolution on the interpretation of satellite NO_2 observations, *Atmos. Chem. Phys.*, *11*, 11647–11655.

Wiedinmyer, C., et al. (2011), The Fire Inventory from NCAR(FINN): A high resolution global model to estimate the emissions from open burning, *Geosci. Model Dev.*, *4*, 625–641.

Zhao, C., and Y. Wang (2009), Assimilated inversion of NO_x emissions over east Asia using OMI NO_2 column measurements, *Geophys. Res. Lett.*, *36*, L06805, doi:10.1029/2008GL037123.

Zhang, Q., et al. (2009), Asian emissions in 2006 for the NASA INTEX-B mission, *Atmos. Chem. Phys.*, 5131–5153.